

Oxidation and hydrogenation of quasicrystals

B.I. Wehner ^{a,*}, J. Meinhardt ^a, U. Köster ^a, H. Alves ^a, N. Eliaz ^b, D. Eliezer ^b

^a Department of Chemical Engineering, University Dortmund, Emil-Figge-Str. 66, AG Werkstoffe und Korrosion, D-44221 Dortmund, Germany

^b Department of Material Engineering, Ben Gurion University of the Negev, Beer Sheva 84105, Israel

Abstract

Quasicrystals are often regarded as Hume–Rothery phases stabilized at different electron concentrations e/a . Concentration changes during oxidation or hydrogenation are expected to displace the electron concentration out of the stability range. Therefore, these processes might be accompanied by phase transformations. Oxidation experiments with $\text{Al}_{63}\text{Cu}_{25}\text{Fe}_{12}$ icosahedral quasicrystals reveal only in the early stages the formation of a smooth oxide layer accompanying reconstruction of the surface. No phase transformation due to oxygen diffusion into the quasicrystalline structure could be detected. During further oxidation the formation of oxide nodules has been observed rather than a homogeneous thickening of the oxide layer. Heterogeneous phase transformation into $\lambda\text{-Al}_3\text{Fe}_4$ indicates additional segregation effects. $i\text{-Zr}_{69.5}\text{Ni}_{12}\text{Cu}_{11}\text{Al}_{7.5}$ quasicrystals can absorb large amounts of hydrogen which leads to an increase of the quasilattice constant by 10% and microstructural changes of so far unknown character: weakening of the contrast of quasicrystals in transmission electron microscopy (TEM) as well as a disappearance of the weak diffraction spots in the corresponding diffraction pattern. © 1997 Elsevier Science S.A.

Keywords: Quasicrystal; Oxidation; Hydrogenation; Zr–Ni–Cu–Al; Al–Cu–Fe

1. Introduction

Quasicrystals possess excellent properties like high hardness, corrosion resistance and a low coefficient of friction; these properties make quasicrystalline coatings very suitable, e.g. for frying pans [1,2]. For application of quasicrystalline material as surface coatings under a variety of environmental conditions oxidation and hydrogenation are of high interest.

From a scientific point of view there is additional interest in these reactions. Quasicrystals are often regarded as Hume–Rothery phases stabilized at different electron concentrations e/a [3]. Concentration changes during oxidation or hydrogenation are expected to displace the electron concentration out of the stability range. Therefore, these processes might be accompanied by a discontinuous or continuous phase transformation.

Only very little information is available on these topics as yet. Some authors report of good oxidation resistance of $i\text{-Al–Cu–Fe}$ quasicrystals in dry air [4]; they do not observe a surface oxide layer but considerable diffusion of oxygen deep into the sample lattice, resulting in an overall oxygen content of nearly 3 at.%.

Ti-based quasicrystals have been demonstrated by Viano et al. [5] to absorb reversibly hydrogen from the gas phase up to a hydrogen to metal atom ratio $\text{H/M} = 1.6$. The aim of this paper is to present our first results on the oxidation and hydrogenation of quasicrystalline alloys.

2. Experimental

The preparation of quasicrystalline Al–Cu–Fe [6] and Zr–Ni–Cu–Al [7] alloys has been described elsewhere in detail. The microstructure was studied by X-ray diffraction (XRD) as well as by TEM using a Philips CM200 electron microscope operating at 200 kV. Surface morphology of the oxidized quasicrystalline alloys was studied by scanning electron microscopy (SEM) using a Hitachi S-4500 operating between 1 and 30 kV. Low-kV operation allows the microscopical study of oxide layers without any additional conducting surface coatings.

Polished bulk samples of quasicrystalline $\text{Al}_{63}\text{Cu}_{25}\text{Fe}_{12}$ were oxidized in air at 780°C up to 336 h using a Netzsch thermal gravimetric analyzer (STA 409) and investigated by XRD, scanning as well as TEM and atomic force microscopy (AFM).

* Corresponding author.

Partial quasicrystalline $Zr_{69.5}Cu_{12}Ni_{11}Al_{7.5}$ was charged electrolytically with hydrogen in a 1:1 glycerine-phosphoric acid electrolyte at a current density of $i = 25 \text{ A m}^{-2}$. The hydrogen content was measured by using a microbalance with an accuracy of $\pm 1 \text{ } \mu\text{g}$. Elongation changes were studied in-situ during the charging using a special strain-gauge device thermal analyzer with a relative sensitivity $\Delta l/l_0 = 2 \times 10^{-7}$. Thermal stability was investigated by means of differential scanning calorimetry (DSC) using a Dupont 910/990 calorimeter.

3. Results and discussion

3.1. Oxidation

We studied the oxidation of quasicrystalline $i\text{-Al}_{63}\text{Cu}_{25}\text{Fe}_{12}$, which is thermodynamically stable between 750 and 850°C [8]. Usually oxygen exhibits different affinities to the elements of an intermetallic compound leading to selective oxidation. Preferred oxidation of aluminum should lead to a change of concentration in the surface near area and should induce a phase transformation of the i -phase into the β -phase [9]. In general oxidation may proceed by two reactions:

- Absorbed oxygen diffuses into the quasicrystal and induces a phase transformation into an oxygen stabilized phase.
- Oxygen reacts at the surface forming metal oxides; the interface zone underneath the oxide layer depletes in the preferentially oxidized element. Thus the concentration is shifted out of the stability range of the quasicrystalline phase and a phase transformation can occur.

After 30 min of oxidation the i -phase shows deep ditches etched at the grain boundaries and a buckled grain surface (see Fig. 1(a)). AFM reveals a surface topography consisting of 200 nm sized islands. These islands probably form the first thin oxide layer of a few tens of nanometers in thickness. After 2 h oxide nodules irregularly distributed over the grain surface can be observed by SEM (Fig. 1(b)); the X-ray diffraction exhibits $\alpha\text{-Al}_2\text{O}_3$ -peaks apart from the characteristic peaks for the i -phase. After oxidizing for 336 h the oxide nodules form a voluminous oxide layer.

Thinned TEM-samples have been oxidized for 10 min for studying the early stages of oxidation microscopically. After such treatment the surface is covered by oxide islands and the i -phase has partially transformed especially in the thinner parts near the rim of the sample into $\lambda\text{-Al}_{13}\text{Fe}_4$ which exhibits a large number of planar defects and twins perpendicular to the growth direction. This phase transformation of $i\text{-Al}_{63}\text{Cu}_{25}\text{Fe}_{12}$ into $\lambda\text{-Al}_{13}\text{Fe}_4$ must be accompanied with a loss of copper. This effect cannot be explained as yet;

it might be due to Cu segregation prior to any oxidation process. Cu segregation for example is known from surface precipitation in Al(Cu) alloys.

All additional peaks in the diffraction pattern which result from the formation of the thin oxide islands can be indexed by $\gamma\text{-Al}_2\text{O}_3$. These oxides formed on the remaining $i\text{-Al}_{63}\text{Cu}_{25}\text{Fe}_{12}$ as well as on the resulting $\lambda\text{-Al}_{13}\text{Fe}_4$ exhibit an orientation relationship (see Fig. 2); in the 5-fold diffraction pattern of the icosahedral phase the additional spots can be assumed to form two cubic (111)-planes turned towards each other about 12°. This means that each cubic (111)-plane of the oxide has one axis together with the 5-fold quasicrystalline pattern. But no evidence for a continuous phase transformation due to diffusion of oxygen into the quasicrystal has been found as yet. The orientation relationship between the oxide islands and $\lambda\text{-Al}_{13}\text{Fe}_4$ is given by $(0\bar{1}0)\text{Al}_{13}\text{Fe}_4 // (111)\text{Al}_2\text{O}_3$; $(111)\text{Al}_{13}\text{Fe}_4 // (\bar{1}10)\text{Al}_2\text{O}_3$.

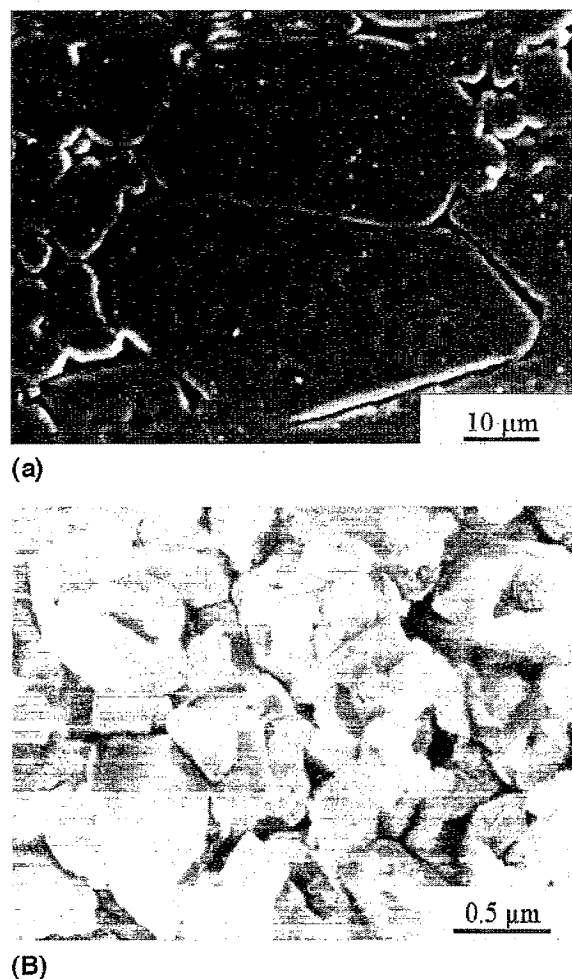


Fig. 1. (a) SEM image of $i\text{-Al}_{63}\text{Cu}_{25}\text{Fe}_{12}$ surface (30 min, 780°C, air). (b) SEM image of oxide nodules on $i\text{-Al}_{63}\text{Cu}_{25}\text{Fe}_{12}$ (2 h, 780°C, air).

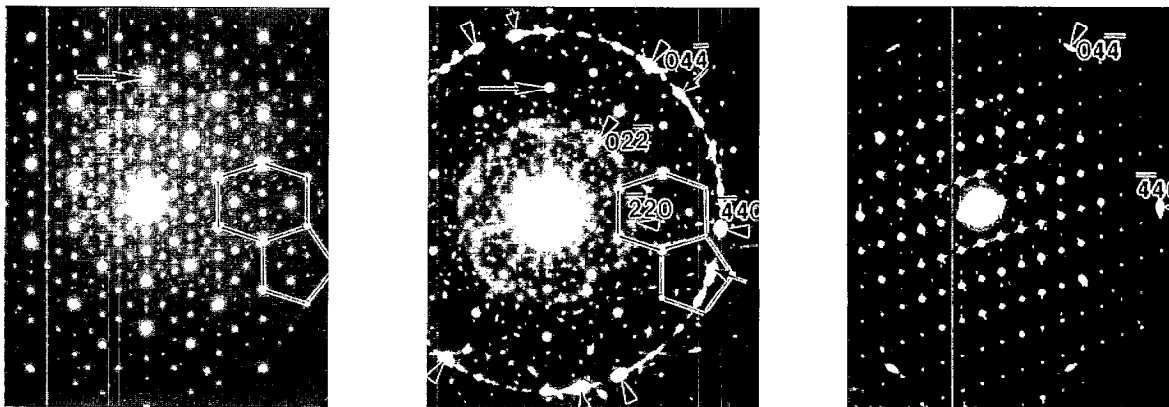


Fig. 2. SAD pattern (a) before oxidation: $i\text{-Al}_{63}\text{Cu}_{25}\text{Fe}_{12}$ 5-fold axis; (b) after 10 min of oxidation: $i\text{-Al}_{63}\text{Cu}_{25}\text{Fe}_{12}$ 5-fold axis; and (c) $(0\bar{1}0)$ $\text{Al}_{13}\text{Fe}_4$.

3.2. Hydrogenation

Samples of quasicrystalline $\text{Zr}_{69.5}\text{Ni}_{12}\text{Cu}_{11}\text{Al}_{7.5}$ ribbons were charged electrolytically up to a maximum hydrogen-to-metal ratio H/M of 1.9; but there is strong evidence that even higher hydrogen contents can be achieved. This is a rather high hydrogen content compared, e.g. with amorphous $\text{Ni}_{25}\text{Zr}_{75}$ or $\text{Cu}_{33}\text{Zr}_{67}$ alloys [10] where the maximum hydrogen content was always related to the ZrH_2 composition. The elongation during hydrogen charging can be used to calculate the partial volume of hydrogen to be about $5 \times 10^{-3} \text{ nm}^3/\text{H-atom}$ which is a rather large value.

As shown in the X-ray diffraction diagram (Fig. 3) the elongation during hydrogenation was accompanied with an increase in the quasilattice constant by about 10% at H/M = 1.9; the amorphous matrix exhibits a similar increase in the nearest neighbor distance. Such an increase compares quite well with the 7% increase as observed in the Ti-based quasicrystals at H/M = 1.6 [5]. By TEM no evidence for the formation of a new

crystalline or quasicrystalline phase has been found. However, in the X-ray as well as electron diffraction pattern of hydrogenated quasicrystals (Figs. 3 and 4) only the strongest peaks are visible; the weaker peaks have disappeared. The volume fraction of the quasicrystals has not changed, but their contrast in bright-field images weakens significantly (see Fig. 5). These effects could result from some kind of defect or phason formation during the hydrogenation. At the moment work is underway to study the involved micromechanism of the continuous structural changes during hydrogenation by TEM in detail.

Thermal stability of the hydrogen charged quasicrystals was investigated by DSC. Whereas, e.g. in Ni–Zr metallic glasses thermal stability deteriorates with increasing hydrogen content, in the quasicrystalline specimen the hydrogen is driven out prior to any other reaction. Annealing of hydrogenated samples (H/M = 1.9) for 4 h at 200°C has been observed to reduce the hydrogen content to H/M = 0.9. DSC runs (20 K min^{-1}) between 50 and 350°C reveal a weak exothermic reaction above 170°C. However, care has to be taken to avoid oxidation of the specimen surface during

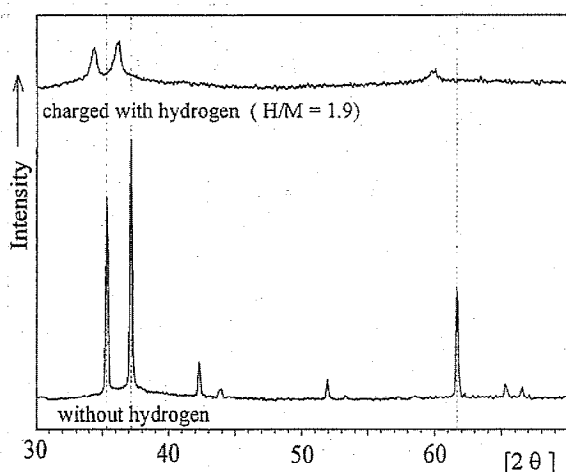


Fig. 3. X-ray diffraction of quasicrystalline $\text{Zr}_{69.5}\text{Ni}_{12}\text{Cu}_{11}\text{Al}_{7.5}$ before and after hydrogen charging.



Fig. 4. Electron micrograph and diffraction pattern of partially hydrogenated quasicrystalline $\text{Zr}_{69.5}\text{Ni}_{12}\text{Cu}_{11}\text{Al}_{7.5}$.

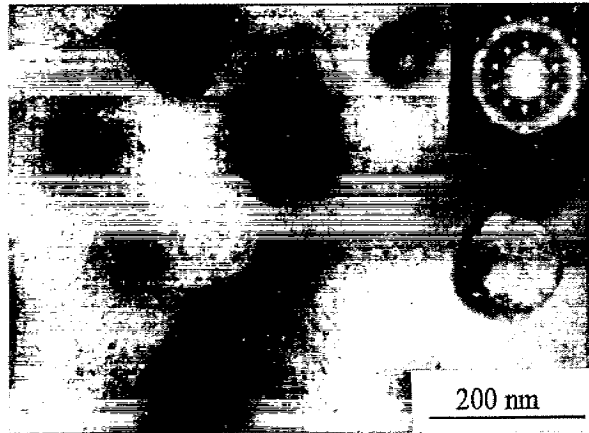


Fig. 5. Electron micrograph and diffraction pattern of partially quasicrystalline $Zr_{69.5}Ni_{12}Cu_{11}Al_{7.5}$ after hydrogen charging ($H/M = 1.9$).

charging or degassing, since even a thin ZrO_2 surface film will act as a barrier for further hydrogen diffusion. After degassing the quasilattice parameter has been restored totally, whereas the weak contrast of the bright-field images of the quasicrystals as well as the lack of the weak diffraction lines still remain, thus indicating the remaining high density of defects.

4. Conclusion

By oxidizing thinned TEM-samples it is possible to observe the very beginning of the oxidation process of icosahedral $Al_{63}Cu_{25}Fe_{12}$ and the involved phase transformations. Oxidation has been found to be accompanied by a phase transformation of the i -phase into the λ - $Al_{13}Fe_4$ -phase. Such a reaction can be understood by assuming Cu segregation which in turn might be responsible for the nodular growth of the oxide. Orientational oxide growth of γ - Al_2O_3 was detected at the surface of oxidized i - $Al_{63}Cu_{25}Fe_{12}$. No evidence for a

phase transformation due to diffusion of oxygen into the quasicrystals could be detected.

Icosahedral $Zr_{69.5}Ni_{12}Cu_{11}Al_{7.5}$ has been observed to absorb large amounts of hydrogen. This reaction is accompanied by a large increase of the quasilattice constant and probably the formation of a high density of defects which leads to a weakened contrast in TEM and the disappearance of the weak diffraction spots. During degassing at temperatures below $400^\circ C$ only the quasilattice constant is restored, but the defects cannot be annealed-out.

Acknowledgements

This work was supported by the Deutsche Forschungsgemeinschaft (DFG Ko 668/19-1). The Minister of Science and Technology of Nordrhein-Westfalen (Germany) has provided the Netzsch thermogravimetric analyzer. The authors are indebted to cand.-Ing. D. Zander for her help in the hydrogenation experiments.

References

- [1] N. Rivier, *J. Non-Cryst. Sol.*, 153/154 (1993) 458.
- [2] S.-S. Kang, J.M. Dubois and J. von Stebut, *J. Mater. Res.*, 8 (1993) 2471.
- [3] P.A. Bancel and P.A. Heiney, *Phys. Rev.*, B33 (1986) 7917.
- [4] S.-S. Kang and J.M. Dubois, *J. Mater. Res.*, 10 (1995) 1071.
- [5] A.M. Viano, R.M. Stroud, P.C. Gibson, A.F. McDowell, M.S. Conradi and K.F. Kelton, *Phys. Rev.*, B51 (1995) 12026.
- [6] U. Köster, H. Liebertz and W. Liu, *Mater. Sci. Eng.*, A181/182 (1994) 777.
- [7] U. Köster, J. Meinhardt, S. Roos and H. Liebertz, *Appl. Phys. Lett.*, 69 (1996) 179.
- [8] J.M. Dubois, C. Janot, C. Dong, M. deBoissieu and M. Audier, *Phase Transitions*, 32 (1991) 3.
- [9] F. Faudot, *Ann. Chim. Fr.*, 18 (1993) 445.
- [10] D. Menzel, A. Niklas and U. Köster, *Mater. Sci. Eng.*, A133 (1991) 312.